Chapter V

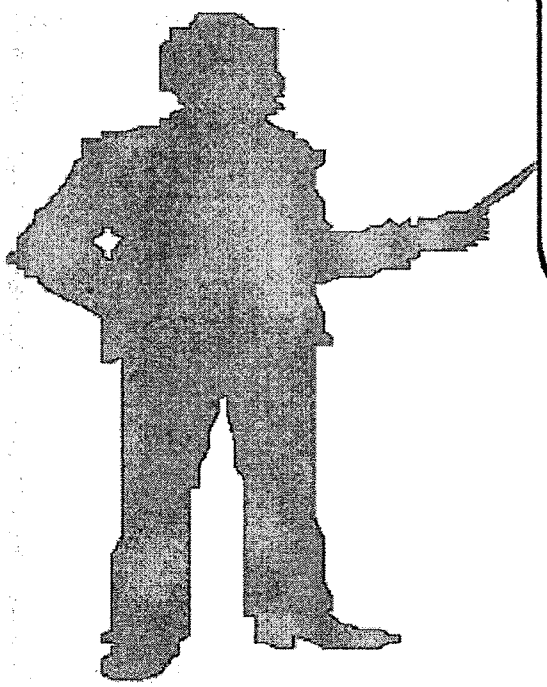

In Vitro Cell Line Studies and Tumor Regression on DMBA Induced Breast Tumor Bearing Rats

5.1. Introduction

Increased attention has been paid to develop vesicular systems based on block copolymers, named polymersomes, as competent drug carrier in recent years, with some remarkable, attractive and feasible characteristics (Discher and Eisenberg 2002; Murali et al., 2008; Upadhyay et al., 2009a). Indeed, polymersome is one of the supramolecular self assembled structures of block copolymer in aqueous and non-aqueous media and has been proved as emerging novel carrier for drug delivery (Discher et al., 2006, Upadhyay et al., 2009b) and gene therapy (Discher et al., 2009). Compared to liposomes, polymersomes have brilliant advantages such as high membrane stability and permeability that can be controlled and modulated by varying block lengths. The control of these properties is mainly correlated to the membrane thickness that can be varied to a larger extent in polymersomes (5-20nm) compare to liposome (3-5nm). These characteristics can overcome most of the stability problems (mainly drug leakage and disintegration of membrane) encountered in lipidic vesicles due to the high fluidity of their bilayers. In addition, it has been evidenced that the release profiles and kinetics of polymersomes can be controlled *in vitro* and *in vivo* (Discher and Eisenberg 2002; Antonietti and Förster 2003). Furthermore, desirable sized polymersomes could be obtained depending on the composition and copolymer chain length, which develop towards smart drug delivery systems (Rodríguez-Hernández et al., 2005; Battaglia et al., 2009)

Here we are presenting the biomedical applications of a new generation of poly(benzyl L-glutamate)-*block*-hyaluronan PBLG-*b*-HYA polypeptide-*block*-polysaccharide copolymers. Hyaluronan is water soluble, non-immunogenic, naturally occurring linear glycosaminoglycan consisting of repeating disaccharide units of d-glucuronic acid and (1-ß-3) N-acetyl-d-glucosamine and having dual characters: it is used as the hydrophilic and stabilizing segment of polymersomes that can simultaneously acts as targeting bio-receptor entity (Upadhyay et al., 2009b). Indeed, because HYA is a major ligand for CD44 receptor, it can be used to target cancer cells which over-express CD44 glycoproteins (Eliaz and Szoka 2001, Khodadadian et al., 2007; Peer and Margalit 2004; Luo and Prestwich 2001).

As per our knowledge, we recently reported for the first time poly(benzyl L-glutamate)-block-hyaluronan block copolymers that formed self-targeted polymersomes having hyaluronan rich surface toward targeting CD44 positive C6 glioma cells (Upadhyay et al., 2009b). However, other research groups worked on the hyaluronan mediated tumor targeting, which include drug conjugation with HYA (Banzato et al., 2008), HYA attached on the preformed liposomes (Peer and Margalit 2004) and micelle based on HYA graft polymer (Lee et al., 2009). Several authors proved the efficacy of HYA targeting in over-expressing CD44 cells and less efficiency in cells having less or no expression of CD44 (Lee et al.,2008; Hyung et al., 2008; Eliaz and Szoka 2001; Eliaz et al., 2004).

In this chapter, we aimed to demonstrate the *in vitro* and *in vivo* efficacy of a formulation of poly(γ-benzyl L-glutamate)-*block*-hyaluronan ($PBLG_{23}$-*b*-HYA_{10}) based polymersomes containing DOX anticancer drug as chemotherapeutic agent. We evaluated the targeting and therapeutic potential of the PolyDOX in cancer cells such as human glioblastoma cell line (U87) (Knüpfer et. al., 1999) and human breast cancer cell line (MCF-7) (CORADINI et al., 1999) expressing different level of CD44 receptors, by assessing *in vitro* drug release kinetics, cell cytotoxicity, cellular uptake efficiency, and ROS to address the concept of self-targeted polymersomes. In addition antitumor activity was investigated on DMBA (7,12-dimethylbenz[α]anthracene) induced breast tumor bearing rats.

5.2. Materials

Dulbecco's Modified Eagles Medium (DMEM), antibiotics (Penicillin G, Streptomycin and Nystatin), DCFH-DA dye and MTT dye were purchased from Sigma (INDIA). Cells from in-house stock in INMAS, Delhi, INDIA.

5.3. Cell culture

The malignant cell lines U87 (human glioma) and MCF-7 (human breast cancer cells) were maintained in low and high glucose Dulbecco's Modified Eagles Medium (DMEM) respectively supplemented with 10% foetal bovine serum and antibiotics (Penicillin G 50000 unit/l. Streptomycin 38850 unit/l and Nystatin 9078 unit/l). Stock culture were

maintained in the exponential growth phase by passaging them every 3 days with their growth medium in 25cm^2 plastic flask (Tarson, Kolkata, India) at 37°C in 5% CO_2/95% air.

5.4. CD44 expression (FACS analysis)

Expression of CD44 hyaluronan receptor level in MCF-7 and U87 cells were investigated by fluorescence activated cell sorter (FACSCalibur, Becton Dickinson, Germany). After rinsing with PBS, 10^5 cells were incubated 45 min at 4°C with anti CD44-labeled PE antibody (4μg). The stained cells were rinsed twice, collected and resuspended in 250 μL PBS and the degree of receptor expression was evaluated by flow cytometry.

5.5. DOX uptake assay

5.5.1 Microscopy

Cells were plated at a density of 0.1 x 10^6 cells/well (40 mm) containing 12mm sterile cover slips for 24h. Free DOX (10μM) and PolyDOX (10μM) were incubated for 3 – 48h at 37°C in 5% CO_2/95% air. After the designated time intervals, the cover slip were removed, washed 2 times with PBS and immediately observed in green light under the fluorescence microscope (Olympus BX60, JAPAN) for uptake. Image acquired at 40x optical zoom.

5.5.2 Flow-cytometric Analysis

Cells were seeded at a density of 0.1 x 10^6 cells per dish (40 mm) for 24 h. Treatment were done with free DOX and PolyDOX at 5 and 10μM DOX concentration for 3 – 24h at 37°C in an atmosphere of 5% CO_2/95% air and then medium was removed and twice cells washed with PBS and collected through centrifugation (1000 rpm for 10 min) at each time point. Cells were resuspended in 250μl PBS before measurements were made. Fluorescence histograms were recorded with a BD FACSCalibur (Beckton Dickinson) flow cytometer and analyzed using Cell Quest software supplied by the manufacturer. Minimums of 10,000 events were analyzed to generate each histogram. The gate was arbitrary set for the detection of green fluorescence (150, FL1-H, 400, 0, FSC, 200, linear scale).

5.6. Chemosensitivity Assay

The cytotoxic effect of free DOX or PolyDOX on the cells was determined by the MTT (3-(4,5-dimethyathiazol-2-yl)-2,5-diphenyl tetrazolium bromide) assay. Cytotoxic effect of DOX and PolyDOX at DOX equivalent concentration from 1 to 20μM was determined for 3-96 h in two ways : (a) immediately processed for drug effect measurement (continuous or immediate effect); or (b) washed, incubated in drug-free medium, and processed for drug effect measurements at 96 h (delayed effect). Samples containing 5000 cells (from an exponentially growing culture) in 200μl aliquots were plated onto 96-well flat-bottomed microtiter plates and incubated for 24h at 37°C in an atmosphere of 5% CO_2/95% air. For the delayed effect, DOX containing medium or PolyDOX containing medium was removed at the end of treatment, and the culture plates were rinsed three times with 200 μl of growth medium. Afterward, cells were incubated with 200μl of drug-free growth medium until 96 h. The immediate effect was determined immediately after drug treatment. The delayed effect was determined at 96h, irrespective of treatment duration. Subsequently after end time points, cells were incubated with 10% MTT (5mg/mL in PBS) in incubator at 37°C for 2h. The cells were lysed and the formazan crystals dissolved using DMSO (150μL) at the end of incubation. The absorbance was noted at 570 nm using 630 nm as reference wavelength on multiwell plate reader (Biotek instruments, USA). Control sample was treated as incubation without DOX and PolyDOX. Absorbance was directly related to % cell viability and control cell viability was considered 100% cell viability at each respective time points:

% cell viability=$\left(\frac{N_t}{N_u}\right)\times 100$, where N_t and N_u are the number of surviving cells in the treated groups with DOX and PolyDOX, and in the untreated group respectively.

5.7. Competitive inhibition of PolyDOX in presence of free hyaluronan

Cells (0.1 x 10^6) per dish (40 mm) in serum free media were incubated with DOX and PolyDOX at 10μM (DOX concentration) together with free HYA (Mw = 5000g/mol) for 1h at concentration 2mg/mL at 37°C. Cells were washed twice with PBS and collected in

the tube by centrifugation (1000 rpm for 10min). Cells were resuspended in 300µl PBS before measurements were made. Samples were acquired on BD FACSCalibur (Beckton Dickinson) flow cytometer and analyzed using Cell Quest software supplied by the manufacturer. For each analysis, at least 10000 events were counted.

5.8. Reactive oxygen Species (ROS) measurement

Cells were seeded at a density of 0.1 x 10^6 cells per dish (40 mm) for 24 h. Cells were incubated with free DOX and PolyDOX at 10µM for 6 and 24h at 37°C in an atmosphere of 5% CO_2/95% air. After the completion of exposure time cells were washed with PBS and incubated for 30 minute with 20 µM DCFH-DA prepared in PBS containing 1mM of each $CaCl_2$ and $MgCl_2$ and 5 mM glucose. Then cells collected in the tube by centrifugation (1000 rpm for 10min). Cells were resuspended in 300µl PBS before measurements were made. Fluorescence histograms were recorded with a BD FACSCalibur (Beckton Dickinson) flow cytometer and analyzed using Cell Quest software supplied by the manufacturer. For each analysis, at least 10000 events were counted.

5.9. *In Vivo* Evaluation of Antitumor Efficacy of PolyDOX

The in vivo efficacy of the PolyDOX was assessed in female Sprague–Dawley (SD) rats. Eight-week-old SD female rats (120-140 g) were used for tumor regression study. DMBA (7,12-dimethylbenz[α]anthracene) was administered orally (soybean oil) to rats in three doses of 45 mg/kg dose at weekly interval to generate the tumor. Drug treatment was given after 10 weeks of the last dose of DMBA. The tumor width (w) and length (l) was recorded with a caliper and tumor size was calculated using the formula ($L \times W^2/2$). All the animal experiments were carried out under the guidelines compiled by CPCSEA (Committee for the Purpose of Control and Supervision of Experiments on Animals, Ministry of Culture, Govt. of India), and all the study protocols were approved by Institutional Animal Ethics Committee before the start of the study (IAEC08/60). After 10 weeks of tumor induction, tumor bearing animals were separated and divided randomly into different treatment groups. Animals were treated with a single 250 µL intravenous injection of 5 mg DOX/kg body weight of PolyDOX, equivalent DOX dose

in PBS for groups A and B, respectively. The control groups C received a single 250 µL intravenous injection of PBS (pH 7.4). The tumor size was calculated as per above mention formula. The study was terminated after 30 days post treatments. Treated tumor bearing rat's survival observation was continued till 60 days post treatments

5.10. Assessment of cardiotoxicity

Sprague–Dawley female rats were used for determination of cardiotoxicity. Free DOX and PolyDOX was administrated by IV route at single dose (5mg/kg body weight). Blood samples were drawn from the retro orbital plexus under light ether anaesthesia, into non-heparinized capillary tubes at 21st day after IV injection of free DOX and PolyDOX. Plasma was separated by centrifugation at 4000 rpm for 5 min and stored at -20^{0}C until analysis. Plasma enzyme activity such as LDH and CPK levels were assayed using commercially available kits, LDH (Crest Biosystem, India) and CK-MB (Diagnosticum, Hungry) based on the method provided by the manufacturer's in instructions supplied with the commercial kits. DOX induces toxicity on cardiac cells and LDH and CPK release from heart and elevated level of these enzymes is directly related to cardiotoxicity of DOX.

5.11. Statistical analysis

All data expressed as means ± standard deviation (S.D.) are representative of at least three or six different experiments. When comparing more than two mean values of groups, a one-way analysis of variance (ANOVA) was performed using KaleidaGraph (Version 4.01) program. To find out whether the two values of interest were significantly different, Post Hoc Test was performed. Difference between two groups was evaluated using Student's t-test. A "P" value less than 0.05 was considered statistically significant.

5.12. Results and Discussion

5.12.1 Analysis of CD44 expression

Both cell lines used for comparative study of DOX and PolyDOX are CD44 expressing (M.M. Knüpfer et al., 1999 and CORADINI et al., 1999) therefore we determined relative CD44 expression to each other in both the cell lines and we observed that both

cells express significant (P<0.05) CD44 receptor compare to unstained of their respective cells. MCF-7 cells were significantly (P<0.001) high (MFI = 227±10.5) CD44 expressing than U87 cells (MFI = 47±5.9) (Figure 5.1 and 5.2).

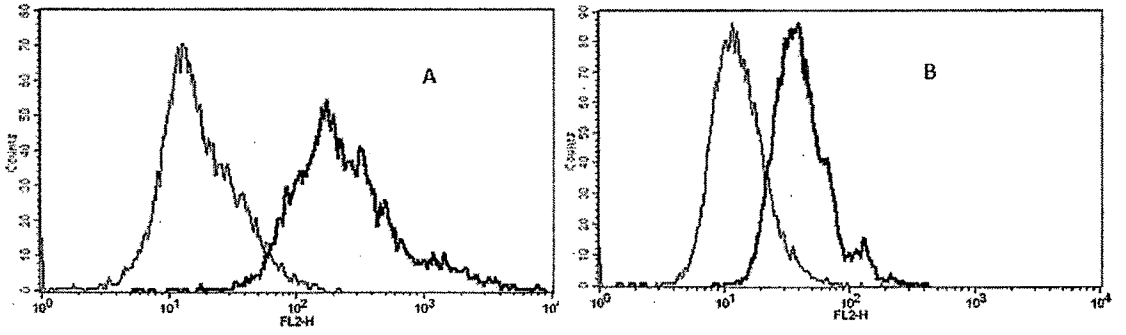

Figure 5.1 CD44 expression of human breast cancer MCF-7 cells (A) and human U87 glioma cell lines (B) measured by flow cytometry. Grey and black lines are representing unstained and stained cells with PE labeled CD44 antibody respectively. (n = 3).

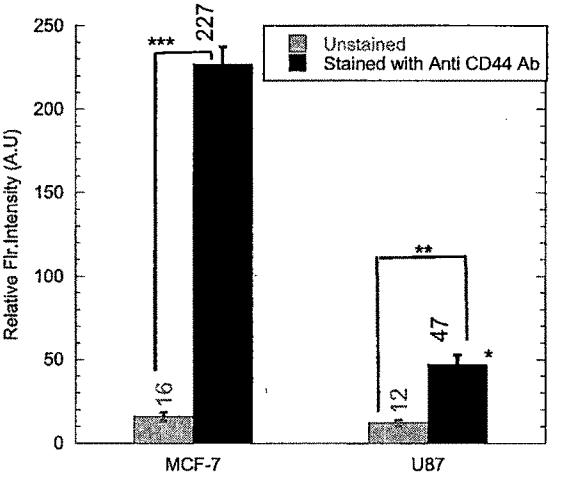

Figure 5.2 Relative fluorescence intensity of unstained and stained cells (MCF-7 and U87) measured by flow cytometry. Grey and black column are representing unstained and stained cells with PE labeled CD44 antibody respectively.
(n = 3, * P<0.001, U87 vs. MCF-7; **P<0.05, ***P<0.001).

5.12.2. Analysis of DOX uptake by fluorescence microscopy

DOX and PolyDOX internalization in the MCF-7 and U87 cells was studied using fluorescence microscopy. Free DOX solution and PolyDOX with an equivalent amount of DOX (10μM) were added to exponentially growing cells for 3h, 6h, 24h and 48h. As shown in figure 5.3, drug intracellular distribution of the PolyDOX is quite different from

that of DOX solution. After 3h of incubation with the DOX solution in MCF-7, strong fluorescence of DOX was observed in cell nuclei in addition to the very weak fluorescence in cytoplasm, suggesting rapid intercalation of intracellular DOX to the chromosomal DNA after passive diffusion into the cells. On the other hand, as shown in figure 5.3, PolyDOX fluorescence was exhibited speckled red dots throughout the cytoplasm as well as very less in nuclei even after 48h, indicating that PolyDOX were initially trapped within endosomal compartments after cellular uptake. These data not only demonstrate that PolyDOX is an efficient vehicle to transport DOX into the cytoplasm, but also suggest that the internalization mechanism of polymersomes is different from that of free DOX. Similar results were reported by Shuai and coworkers in MCF-7 cells incubated with PEG-*b*-PCL micelles (Shuai et al., 2004) and by Zheng and coworkers, in the Hela and HepG2 cells with amphiphilic graft polyphosphazenes based polymeric micelles (Zheng et al., 2009). In addition, Maysinger group reported in Science and have demonstrated localization of polymeric micelles in several cytoplasmic organelles, including mitochondria, but not in the nucleus. They also evidenced that micelles changed the pattern of cellular distribution and increased the amount of the agent delivered to the cells (Savic et al., 2003). Finding of these reports and above experimental results, that demonstrated noticeable difference in sub-cellular distribution of DOX, suggested that PolyDOX were taken up by cells mainly via an endocytic pathway (Xiong et al., 2008; Xiong et al., 2007; Lee et. al., 2008) and were then localized in acidic endocytic compartments (i.e. endosomes and later lysosomes). DOX extraction from PolyDOX will be released in a controlled manner from inside endosomes/lysosomes because the *in vitro* DOX release from the PolyDOX was a relatively slow process even at pH 5.5 (Chapter IV).

Furthermore, the presence of p-glycoprotein pump (Pgp) expelled DOX from U87 cells (Rittierodt and Harada 2003). Indeed, a decrease of DOX fluorescence was observed in nuclei and cytoplasm of U87 cells after 48h incubation time, whereas remarkable increase in the PolyDOX fluorescence from the cytoplasm was observed as in the case of MCF-7 cells. It has been reported that block copolymer can reversal in multidrug resistance (MDR) occurred by Pgp in tumor cells via direct and indirect inhibition mediated by copolymer and P-glycoprotein (Pgp) interactions or adenosine triphosphate

(ATP) depletion, respectively, as well as damage to the membrane barrier caused by copolymer insertion into the membrane (Hugger et al., 2002; Kabanov et. al., 2002 and Sommer et. al., 2008). Therefore, PolyDOX was able to enhance intracellular level of DOX in Pgp positive U87 cells by above mention mechanisms.

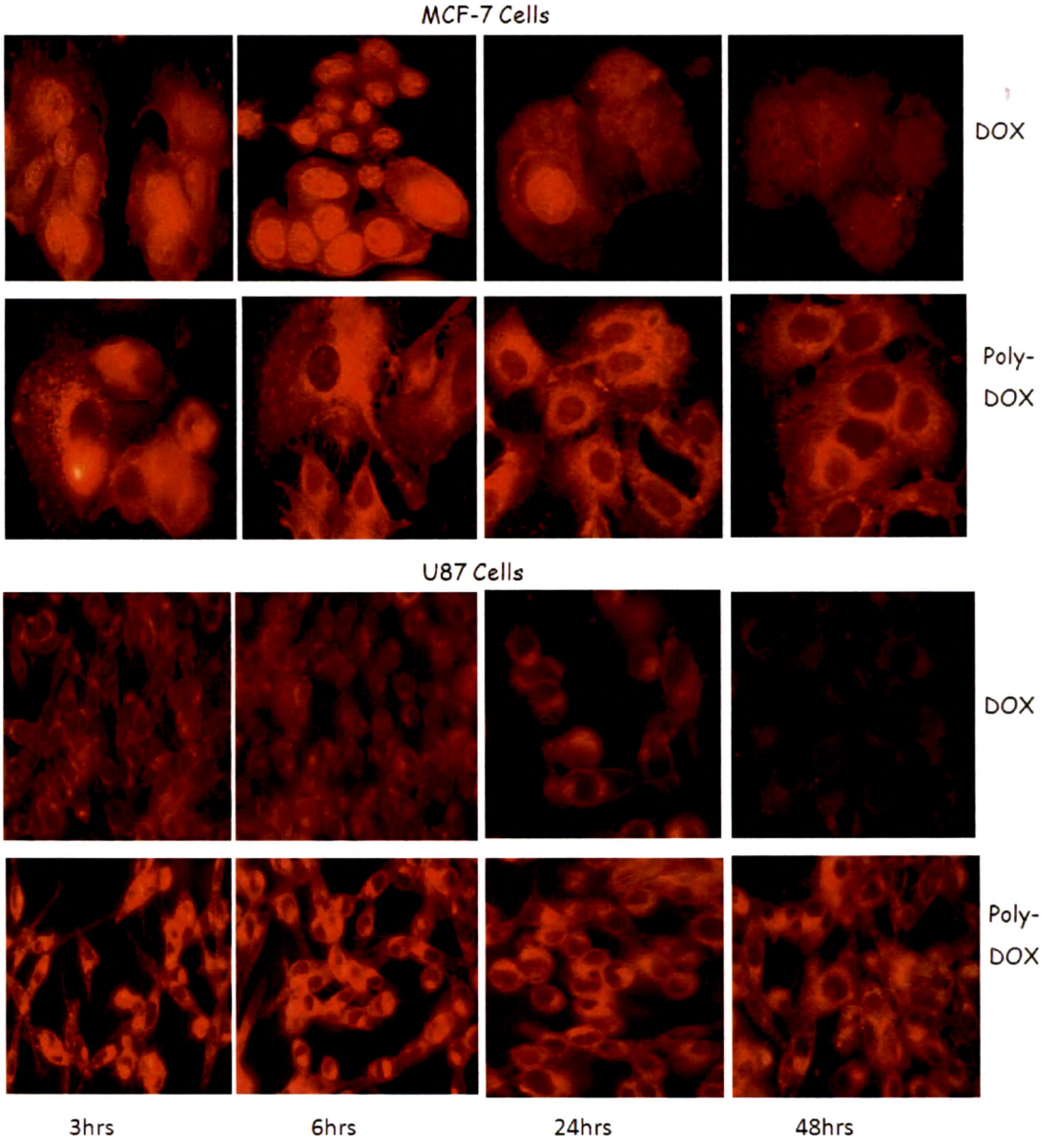

Figure 5.3 Fluorescence microscopy images of DOX and PolyDOX uptake in MCF-7 and U87 cells at 3, 6, 24 and 48h incubation times. (Magnification ×40)

5.12.3. *Analysis of DOX uptake by flow cytometry*

Flow cytometry can also be used for quantitative determination of DOX uptake in cells (Prabaharan et. al., 2009; Zheng et al., 2009). Indeed, since DOX itself is fluorescent, it was used directly to measure cellular uptake without additional markers, fluorescence intensity being directly proportional to the amount of DOX internalized. MCF-7 and U87 cells were incubated at 3h, 6h, and 24h with the DOX and PolyDOX solutions with equivalent DOX concentrations (5μM and 10 μM). DOX fluorescence in cells at different time points were recorded and cells without any DOX treatment were used as a negative control. The results shown in Figure 5.4 indicate that the DOX were successfully transported into cells by being loaded in polymersomes. The cellular uptake of DOX was significantly ($P<0.01$) higher in the samples incubated with PolyDOX than in those treated with free DOX in both MCF-7 and U87 cells, and was concentration dependent. Additionally, the multi-drug resistance (MDR) effect might play a role in reducing the accumulation of free DOX within cells because some amount of MDR proteins is always present in cancer cells. Therefore, free DOX molecules transported within cells are likely to be pumped back out of the cytosol by the p-glycoprotein pump expressed in the membrane of cancerous cells (Coley H et al., 1993). From this standpoint, cellular delivery of DOX from PolyDOX is an attractive way to circumvent the MDR effect which can further potentiate the effects of drugs.

Interestingly, compared with control of their respective cells, PolyDOX was intracellularly significantly ($P< 0.001$) more accumulated in MCF-7 than U87 cells. This notable difference suggests the higher intracellular DOX concentration in PolyDOX incubated cells, can be the result of a higher CD44 expression level in MCF-7 cells. Thus, the enhanced uptake of PolyDOX can be attributed to their facilitated CD44 receptor mediated endocytotic transport, relative to a more passive and less efficient endocytosis pathway in the case of U87 cell lines.

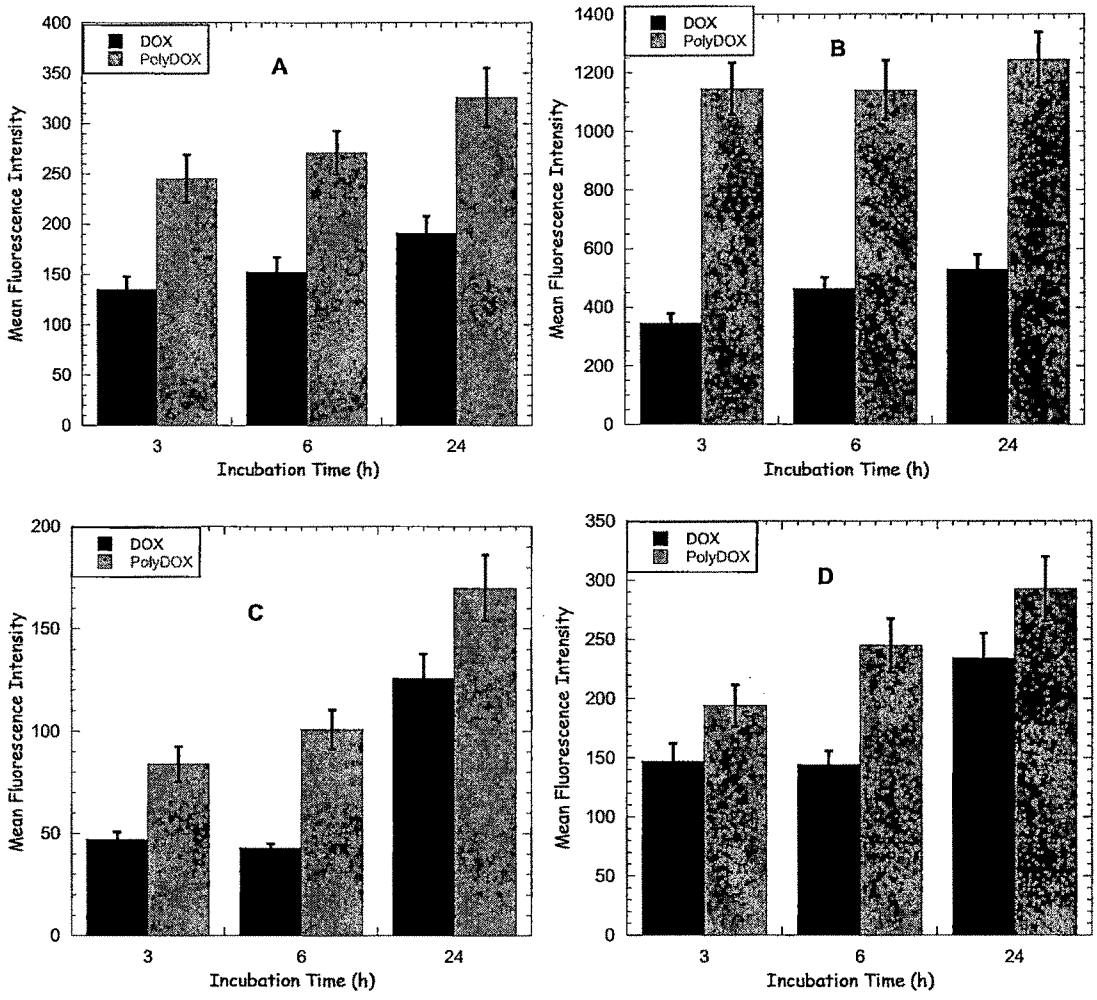

Figure 5.4 (A) and (B) DOX and PolyDOX uptake in MCF-7 cell at 5 and 10 µM DOX concentration respectively. (C) and (D) DOX and PolyDOX uptake in U87 cell at 5 and 10 µM DOX concentration respectively. Data represent mean ± SD (n = 3).

To further confirm whether the PolyDOX were taken up by cells via HYA-specific receptor mediated endocytosis, a competitive inhibition experiment was performed by adding free HYA in the incubating media in order to some extent block HYA receptors on the surface of MCF-7 and U87cells. In both cells, presence of free HYA significantly ($P< 0.01$) reduces MFI (mean fluorescence intensity) of PolyDOX compare to free DOX (Figure 5.5 and 5.6). Figure 5.6A and B shows interfere and reduced DOX fluorescence intensity in PolyDOX incubated cells in presence of free HYA but almost no effect ($P>0.05$) in free DOX uptake. These results demonstrate the role of HYA receptor-

mediated endocytosis in efficient intracellular delivery of hyaluronan based polymersomes.

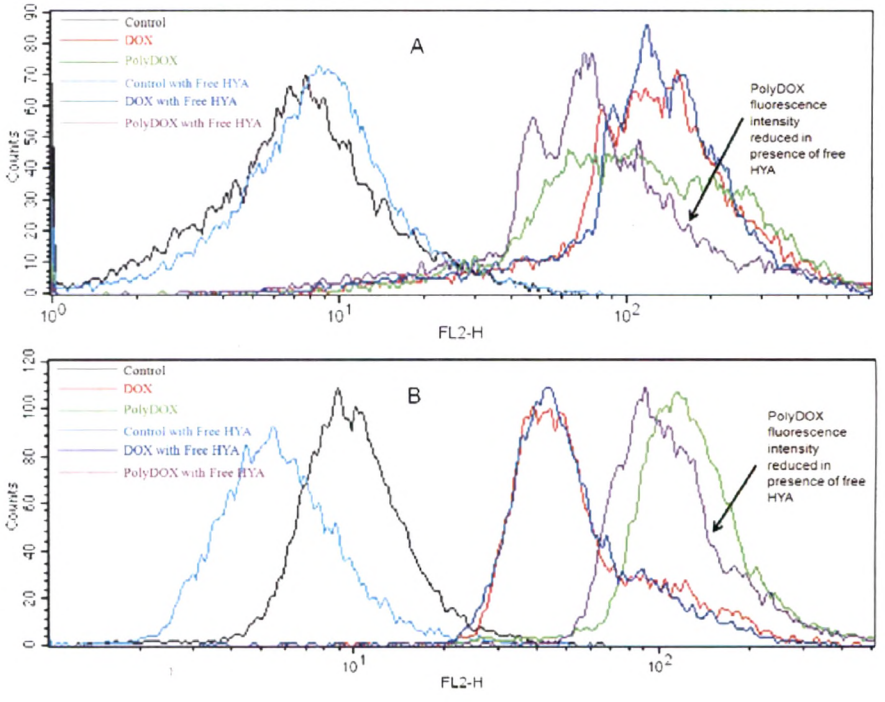

Figure 5.5 (A) and (B) flow-cytometric analysis of DOX (10μM) and PolyDOX (10μM) uptake in presence of free HYA (2mg/mL) in MCF-7 and U87 respectively.

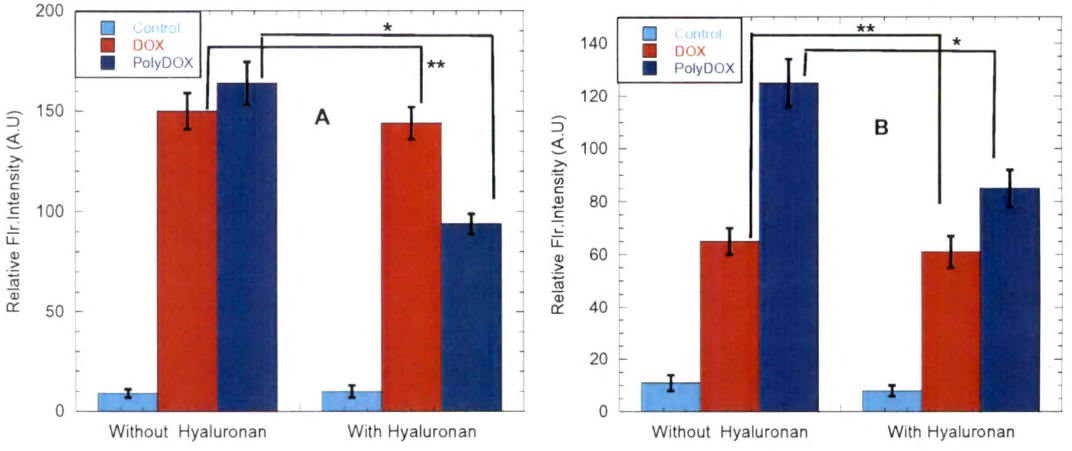

Figure 5.6 (A) and (B) shows flow-cytometric analysis of DOX and PolyDOX uptake and effect of added free HYA (2mg/mL) on uptake of DOX and PolyDOX in MCF-7 and U87 respectively. (*P<0.01, **P>0.05).

5.12.4. Cytotoxicity Study

In vitro cytotoxic effects of the drug and formulation were analyzed using MTT assay. Figure 5.7 shows the viability (%) of MCF-7 and U87cells treated with control empty $PBLG_{23}$-*b*-HYA_{10} polymersomes. It was revealed that the non-loaded copolymer vesicles had nearly no influence to the viability of both cells in the concentration range from 150 to 650 μg/mL, cell viabilities being all above 90%.

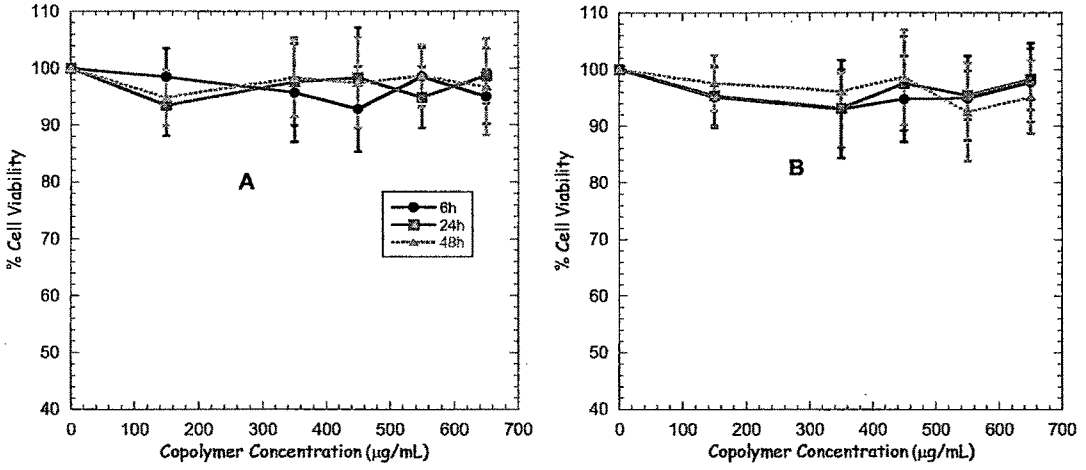

Figure 5.7 (A) and (B) represent % cell viability of MCF-7 and U87 against $PBLG_{23}$-*b*-HYA_{10} copolymer vesicles respectively. Data represent mean ± SD (n = 6).

We investigated the concentration effect of DOX on the viability of cells that are positive for CD44 glycoprotein receptor for hyaluronan with high expression (MCF-7) and low expression (U87). Two approaches have been used, so called immediate effect (continuous exposure effect) and delay effect (Eliaz et al., 2004), referring respectively to the DOX effect that was measured immediately after end of treatment, and measured after an additional growth period after DOX removal from the medium. Immediate effect and the delayed effect at 96h are the same for the 96h exposure.

In both cases, cytotoxicity was concentration and exposure time dependent and cytotoxicity increases with increasing DOX concentration and exposure time for both free DOX and PolyDOX incubation (Figure 5.8 and 5.9). The IC_{50} values calculated from dose response curve (Figure 5.8 and 5.9) are summarized in Table 2.

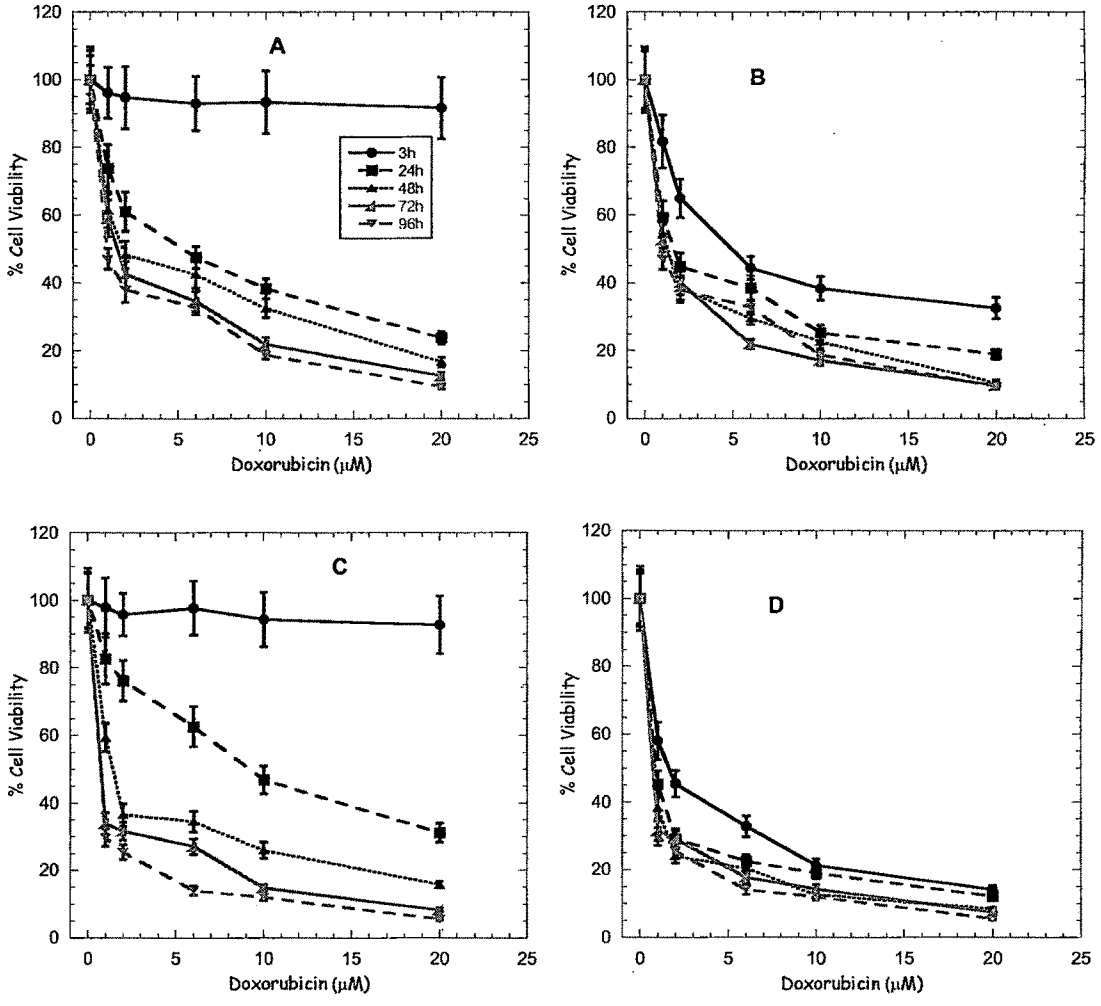

Figure 5.8 (A, B) is the % cell viability with DOX and (C, D) is the % cell viability of PolyDOX incubation in MCF-7 cells at different time points (3-96h). (A and C) represent continuous effect experiment and (B and D) represent delay effect experiment. Data represent mean ± SD (n = 6).

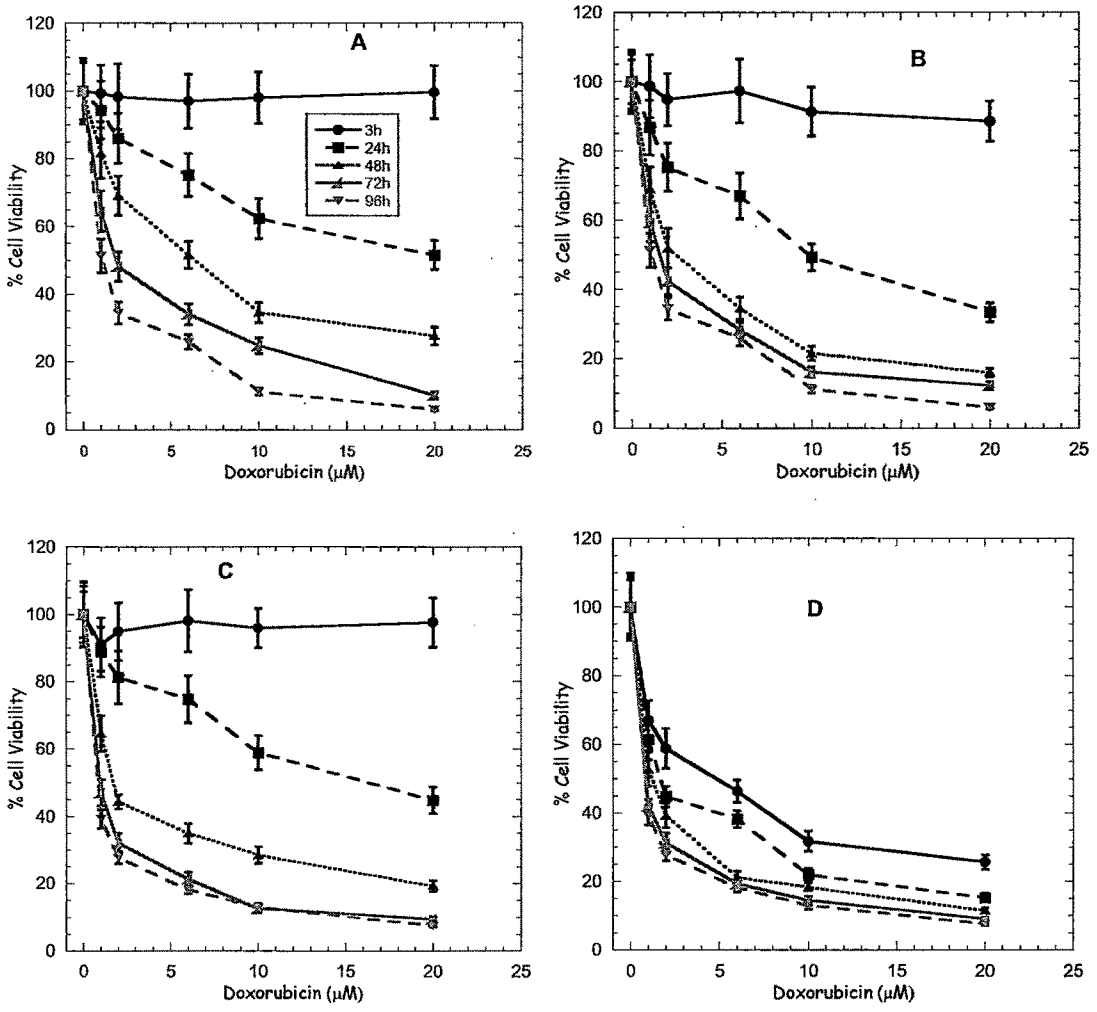

Figure 5.9 (A, B) is the % cell viability with DOX and (C, D) is the % cell viability with PolyDOX incubation in U87 cells at different time points (3-96h). (A and C) represent continuous effect experiment and (B and D) represent delay effect experiment. Data represent mean ± SD (n = 6).

Table 5.1 *In Vitro* Cytotoxicity of PolyDOX and Free DOX (Concentration in μM), IC_{50}#

Exposure time	MCF-7				U87			
	Immediate effect		*Delay effect*		*Immediate effect*		*Delay effect*	
	DOX	PolyDOX	DOX	PolyDOX*	DOX	PolyDOX	DOX	PolyDOX*
3h	>20	>20	5.27	1.63**	>20	>20	>20	3.6**
24h	4.52***	9.13	1.78	0.58	>20	17.0	10.4	1.86**
48h	2.29	1.39	1.20	0.39	5.64	2.04	2.43	1.12
72h	1.60	0.30	1.15	0.255	2.09	0.80	1.52	0.59
96h	0.91	0.24	0.911	0.242	1.03	0.48	1.03	0.48

#IC_{50} inhibitory concentration of DOX producing 50% of cell growth. *P < 0.01, PolyDOX vs. DOX in delay effect experiments. **P < 0.001, PolyDOX vs. DOX. ***P < 0.001, DOX vs. PolyDOX.

DOX and PolyDOX did not show cytotoxicity at 3h in immediate effect experiment in both cells it could be the lag phase (Eliaz et al., 2004) of DOX and PolyDOX, but produced cytotoxicity at 3h in delay effect experiment except in U87cells where DOX expelled from U87 cells (Figure 5.3) due to presence of Pgp pumps (Rittierodt and

Harada 2003). DOX was potent (IC_{50} = 4.52μM) at 24h than PolyDOX (IC_{50} = 9.13μM) but less potent after 48h with continuous exposure (immediate effect) in MCF-7 cells, might be because DOX was in free form and accumulate rapidly in nucleus (Figure 5.3) whereas PolyDOX releases DOX from cytosolic compartments in controlled manner (Figure 5.3) and continuously produced more cytotoxicity at 48, 72 and 96h. PolyDOX was revealed more potent at each exposure time points (3-96h) than free DOX in delay effect experiment in both cells.

The IC_{50} values of PolyDOX were less in each time points either its immediate effect experiment or delay effect experiment in MCF-7 cells than U87 cells. It is clear from the obtained IC_{50} values that PolyDOX was cytotoxic in both CD44 receptor expressing cells (MCF-7 and U87) and more precisely high potent in MCF-7 than U87 by factor of 1.5 at 48h in immediate effect experiment and by factor of 3.2 at 24h in delay effect experiment. It could be due to difference in CD44 receptor level in both cells therefore PolyDOX enhanced high accumulation of DOX intracellularly via highly expressed CD44 mediated endocytosis in MCF-7.

5.12.5. DOX induced Reactive Oxygen Species (ROS) generation

Though DOX is known as DNA damaging anticancer drug acting in cells nuclei, its mechanism of cytotoxicity is not very clear. Some reports suggest that DOX induces calcium release from internal stores leading to generation of ROS that can cause cell death either by disturbing the cellular redox balance or by damaging the DNA (Shadle et al., 2000 and Kim et al., 2006). As observed by fluorescence microscopy (Figure 5.3) of PolyDOX uptake in MCF-7 and U87 cells, the DOX concentration in nuclei was much lower than that for cells incubated with free DOX, which suggest that cytotoxicity due to DNA damage will be less prominent in PolyDOX incubated cells. However, the observed toxicity in PolyDOX incubated cells was interestingly more important than the free DOX treated cells. Therefore, to find out the role of ROS induced cytotoxicity in free and DOX-loaded vesicles treated cells, we determined the ROS level in both cells at 6h and 24h time point (Figure 5.10).

ROS can be simply defined as oxygen containing oxidizing agents and in general, describe the varieties of oxygen-containing species that are inevitably generated during

cellular metabolism (Klaunig and Kamendulis 2004; Shi et al., 2004). ROS are generally divided into two subgroups; free radicals such as superoxide radicals O_2^- and non-radical such as hydrogen peroxide (H_2O_2). ROS, due to their highly reactive nature, possess higher reactivity than molecular oxygen that can damage DNA, proteins, and lipids (Thannickal and Fanburg 2000). Under normal conditions, cells utilize antioxidative or defense systems to balance these toxic products to keep the cells in a state of redox homeostasis.

Surprisingly, PolyDOX increased significantly ($P<0.001$) ROS level in both cell lines compared to free DOX at 24h, and DOX mediated ROS level was also significant ($P<0.05$) compare to control cells (without treatment) because DOX is well known for induction of ROS generation (Gouaze et al., 2001, Beillerot et el., 2008) (Figure 5.10). Therefore, now predictable death mechanism for PolyDOX could be that PolyDOX was more accumulated intracellularly in endosomal, lysosomal and mitochondrial compartments after receptor mediated endocytosis, where it released DOX in a controlled manner and generated ROS level which is directly related to the cellular death.

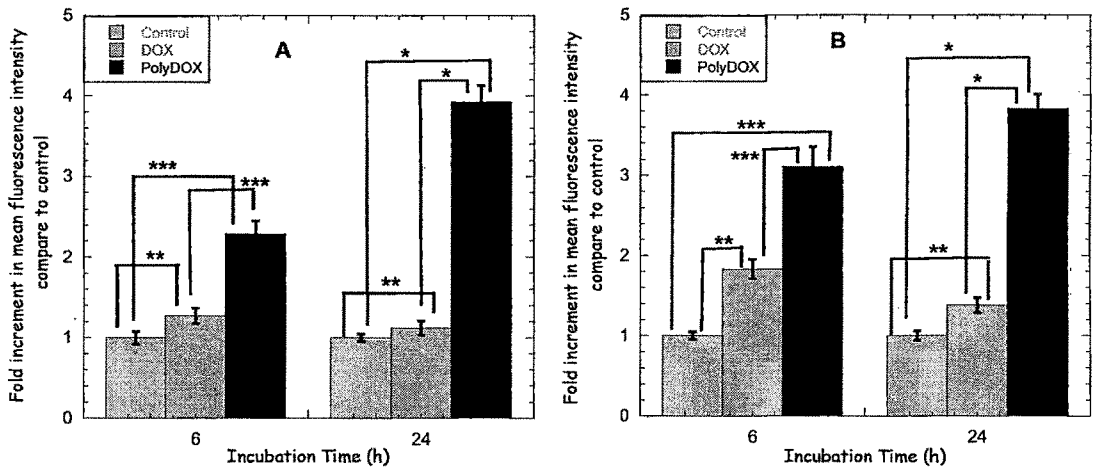

Figure 5. 10 (A) and (B) ROS level in MCF-7 and U87 respectively compare to their control after treatment with DOX and PolyDOX at 6 and 24h. Data represent mean ± SD (n = 3). (*P<0.001, **P<0.05, ***P<0.01).

5.12.6. *Anti-tumor activity of PolyDOX*

Antitumor activities of the PolyDOX was evaluated in DMBA-induced rat breast cancer model (six per group) after a single intravenous injection at dose of 5 mg DOX/kg body

weight. As shown in Figure 5.11A, free DOX and PolyDOX suppressed significantly tumor growth as compared to PBS control group. However, PolyDOX showed higher tumor suppression than the free DOX ($P<0.05$). The high antitumor activity of the PolyDOX can be attributed to a higher accumulation in cancer cells, a controlled release feature and a decreased influence of MDR effect, as suggested earlier. Figure 5.11B represents the DMBA tumor burden on rats after 30 days from the 1st day of drug treatment. Almost negligible tumor burden was achieved after treatment with PolyDOX compare to control and free DOX treatment. Kaplan-Meier survival curve (Figure 5.12) shown after IV injection of PolyDOX enhanced survival time for tumor bearing rats and no mortality was observed after 60 days post treatment. Such observations are also consistent with a higher accumulation of the drug in a more selective manner in cancer cells when animal were treated with PolyDOX, compared to free DOX, allowing a higher efficacy and a reduction of side effects.

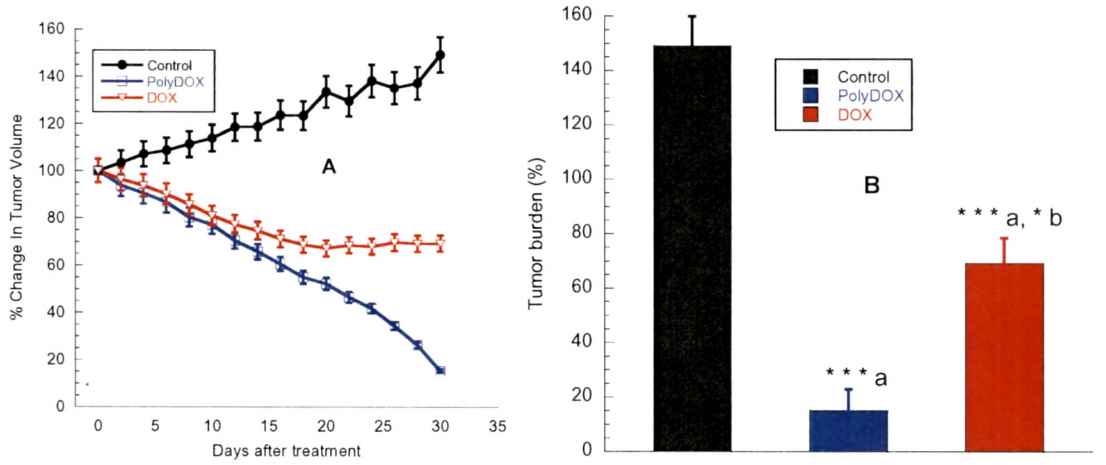

Figure 5.11 (A) Tumor progression after single administration of free DOX and PolyDOX (5 mg/Kg). (B) Comparative tumor burden after 30 days of PolyDOX and free DOX administration in DMBA breast cancer animals. Tumor volume was taken as 100% at the start of drug treatment and tumor progression monitored till the end of the study. Each data point is represented as mean ± SEM (n=6). ***P<0.001, *P<0.05, a vs. control and b vs. PolyDOX.

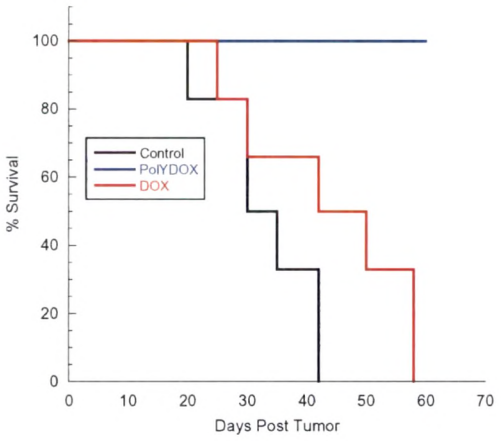

Figure 5.12 Kaplan-Meier survival curve of tumor bearing rat treated with DOX and PolyDOX at dose 5mg/kg equivalent to DOX. Each data point is represented as mean ± SEM (n=6).

In addition, DOX mediated induction in serum enzymes (LDH and CPK) was low after encapsulation in polymersomes compares to free DOX (Figure 5.13A and B). Therefore, reduce level of LDH and CPK by PolyDOX formulation indicates reduce cardiotoxicity of DOX after encapsulation in polymersomes, in agreement with a significant reduction of side-effects and mortality.

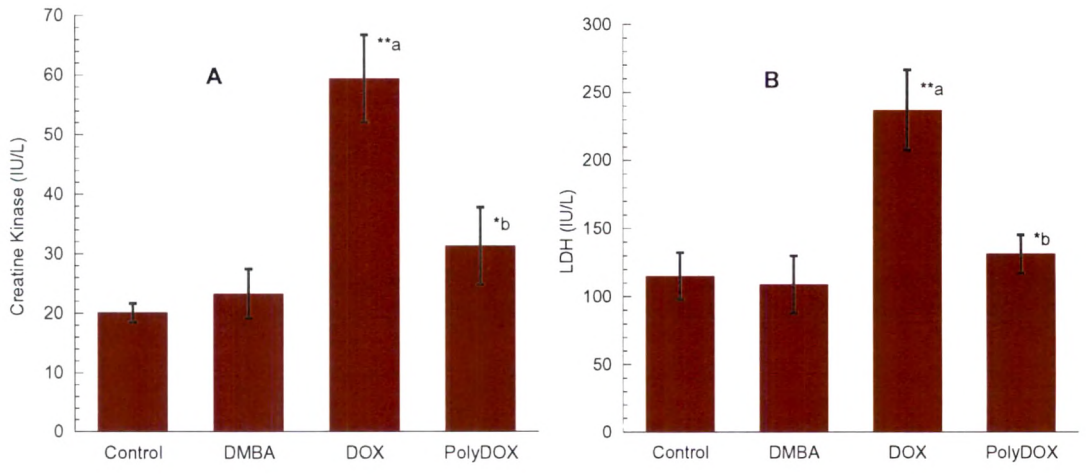

Figure 5.13 (A) Serum creatine kinase levels and (B) lactate dehydrogenase (LDH) levels after DOX and PolyDOX administration in DMBA induced breast cancer animals. Each data point is represented as mean ± SEM. **P<0.01, *P<0.05, a vs. DMBA, control and b vs. free DOX group (n=6)

5.13. Conclusion

Fluorescence microscopy and flow cytometry data demonstrated that DOX was efficiently delivered intracellularly in both cell lines, but to a larger extent in MCF-7 cells, probably due to their higher expression level of CD44 receptors compared to U87 cells. The evidence of the CD44-HYA ligand-receptor interaction as a key parameter influencing the internalization mechanism of PolyDOX was addressed by competitive experiments, where cells were incubated in the presence of free HYA. The significant uptake reduction proved that part of the mechanism for PolyDOX internalization was mediated via CD44 receptor. In addition, cytotoxicity data suggested that after internalization of PolyDOX, DOX released in a controlled manner and produced more cytotoxicity at 3-96h in delay experiment whereas free DOX was more potent at 24h than PolyDOX in MCF-7 cell in continuous exposure experiment. Due to difference in CD44 expression level in both cells, PolyDOX showed more cytotoxicity in MCF-7 cells than U87 cells at each time point and in both types of experiments. In addition, increase level of ROS after PolyDOX incubation suggested prominent death mechanism by being present in cytoplasm and continuously producing ROS, leading to delayed accumulation of ROS. Moreover, PolyDOX efficiently suppressed tumor growth in rats, as compare to DOX with higher survival scores (0% mortality). Also, DOX mediated increase level in serum enzymes that is responsible for DOX mediated cardiotoxicity, was significantly lower after being loaded in polymersomes. Based on all these experimental support, one can conclude that hyaluronan based polymersomes efficiently delivered DOX intracellularly in CD44 expressing cancer cells, inducing a higher toxicity together with a reduction of side effects. These data are in agreement with a selective and high accumulation in cancer cells, probably due to combined enhanced permeation retention (EPR) and more selective receptor mediated endocytosis (RME) effects. Such an approach, where polymersomes can efficiently load hydrophilic and hydrophobic drugs, with a targeting moiety directly integrated in their native constructions, constitute an elegant and efficient therapeutic strategy that will be further addressed in coming chapter.

References

- Ahmed F, Pakunlu RI, Srinivas G, Brannan A, Bates F, Klein ML, Minko T, Discher DE. Shrinkage of a rapidly growing tumor by drug-loaded polymersomes: pH-triggered release through copolymer degradation. Mol Pharm 2006;3(3):340-50.
- Antonietti M, Förster S. Vesicles and Liposomes: A Self-Assembly Principle Beyond Lipids, Advanced Materials 2003;15(16):1323-33.
- Auzenne E, Ghosh SC, Khodadadian M, Rivera B, Farquhar D, Price RE, Ravoori M, Kundra V, Freedman RS, Klostergaard J. Hyaluronic acid-paclitaxel: antitumor efficacy against CD44(+) human ovarian carcinoma xenografts. Neoplasia 2007;9(6):479-86.
- Banzato A, Bobisse S, Rondina M, Renier D, Bettella F, Esposito G, Quintieri L, Meléndez-Alafort L, Mazzi U, Zanovello P, Rosato A. A paclitaxel-hyaluronan bioconjugate targeting ovarian cancer affords a potent in vivo therapeutic activity. Clin Cancer Res 2008;14(11):3598-606.
- Beillerot A, Domínguez JC, Kirsch G, Bagrel D. Synthesis and protective effects of coumarin derivatives against oxidative stress induced by doxorubicin. Bioorg Med Chem Lett 2008;18(3):1102-5.
- Coley HM, Twentyman PR, Workman P. The efflux of anthracyclines in multidrug-resistant cell lines. Biochem Pharmacol 1993;46(8):1317-26.
- Coradini D, Pellizzaro C, Miglierini G, Daidone MG, Perbellini A. Hyaluronic acid as drug delivery for sodium butyrate: improvement of the anti-proliferative activity on a breast-cancer cell line. Int J Cancer 1999;81(3):411-6.
- Discher DE, Eisenberg A. Polymer vesicles. Science 2002;297(5583):967-73.
- Eliaz RE, Nir S, Marty C, Szoka FC Jr. Determination and modeling of kinetics of cancer cell killing by doxorubicin and doxorubicin encapsulated in targeted liposomes. Cancer Res 2004;64(2):711-8.

- Eliaz RE, Szoka FC Jr. Liposome-encapsulated doxorubicin targeted to CD44: a strategy to kill CD44-overexpressing tumor cells. Cancer Res 2001;61(6):2592-601.
- Gouaze V, Mirault ME, Carpentier S, Salvayre R, Levade T, Andrieu-Abadie N. Glutathione peroxidase-1 overexpression prevents ceramide production and partially inhibits apoptosis in doxorubicin-treated human breast carcinoma cells. Mol Pharmacol 2001;60(3):488-96.
- Hearnden V, Lomas H, Macneil S, Thornhill M, Murdoch C, Lewis A, Madsen J, Blanazs A, Armes S, Battaglia G. Diffusion studies of nanometer polymersomes across tissue engineered human oral mucosa. Pharm Res 2009;26(7):1718-28.
- Hugger ED, Novak BL, Burton PS, Audus KL, Borchardt RT. A comparison of commonly used polyethoxylated pharmaceutical excipients on their ability to inhibit P-glycoprotein activity in vitro. J Pharm Sci 2002;91(9):1991-2002.
- Hyung W, Ko H, Park J, Lim E, Park SB, Park YJ, Yoon HG, Suh JS, Haam S, Huh YM. Novel hyaluronic acid (HA) coated drug carriers (HCDCs) for human breast cancer treatment. Biotechnol Bioeng 2008;99(2):442-54.
- Kabanov AV, Batrakova EV, Alakhov VY. Pluronic block copolymers for overcoming drug resistance in cancer. Adv Drug Deliv Rev 2002;54(5):759-79.
- Kim SY, Kim SJ, Kim BJ, Rah SY, Chung SM, Im MJ, Kim UH. Doxorubicin-induced reactive oxygen species generation and intracellular Ca2+ increase are reciprocally modulated in rat cardiomyocytes. Exp Mol Med 2006;38(5):535-45.
- Kim Y, Tewari M, Pajerowski JD, Cai S, Sen S, Williams J, Sirsi S, Lutz G, Discher DE.Polymersome delivery of siRNA and antisense oligonucleotides. J Control Release 2009;134(2):132-40.
- Klaunig JE, Kamendulis LM. The role of oxidative stress in carcinogenesis. Annu Rev Pharmacol Toxicol 2004;44:239-67.
- Knüpfer MM, Poppenborg H, Hotfilder M, Kühnel K, Wolff JE, Domula M. CD44 expression and hyaluronic acid binding of malignant glioma cells. Clin Exp Metastasis 1999;17(1):71-6.

- Lee H, Ahn CH, Park TG. Poly[lactic-co-(glycolic acid)]-grafted hyaluronic acid copolymer micelle nanoparticles for target-specific delivery of doxorubicin. Macromol Biosci 2009;9(4):336-42.
- Lee H, Lee K, Park TG. Hyaluronic acid-paclitaxel conjugate micelles: synthesis, characterization, and antitumor activity. Bioconjug Chem 2008;19(6):1319-25.
- Lee Y, Park SY, Mok H, Park TG. Synthesis, characterization, antitumor activity of pluronic mimicking copolymer micelles conjugated with doxorubicin via acid-cleavable linkage. Bioconjug Chem 2008;19(2):525-31.
- Levine DH, Ghoroghchian PP, Freudenberg J, Zhang G, Therien MJ, Greene MI, Hammer DA, Murali R. Polymersomes: a new multi-functional tool for cancer diagnosis and therapy. Methods 2008;46(1):25-32.
- Luo Y, Prestwich GD. Hyaluronic acid-N-hydroxysuccinimide: a useful intermediate for bioconjugation. Bioconjug Chem 2001;12(6):1085-8.
- Peer D, Margalit R. Loading mitomycin C inside long circulating hyaluronan targeted nano-liposomes increases its antitumor activity in three mice tumor models. Int J Cancer 2004;108(5):780-9.
- Peer D, Margalit R. Tumor-targeted hyaluronan nanoliposomes increase the antitumor activity of liposomal Doxorubicin in syngeneic and human xenograft mouse tumor models. Neoplasia 2004;6(4):343-53.
- Prabaharan M, Grailer JJ, Pilla S, Steeber DA, Gong S. Folate-conjugated amphiphilic hyperbranched block copolymers based on Boltorn H40, poly(L-lactide) and poly(ethylene glycol) for tumor-targeted drug delivery. Biomaterials 2009;30(16):3009-19.
- Rittierodt M, Harada K. Repetitive doxorubicin treatment of glioblastoma enhances the PGP expression--a special role for endothelial cells. Exp Toxicol Pathol 2003;55(1):39-44.

- Rodríguez-Hernández J, Chécot F, Gnanou Y, Lecommandoux S. Toward 'smart' nano-objects by self-assembly of block copolymers in solution. Progress in Polymer Science 2005;30(7):691-24.
- Savic R, Luo L, Eisenberg A, Maysinger D. Micellar nanocontainers distribute to defined cytoplasmic organelles. Science 2003;300(5619):615-8.
- Shadle SE, Bammel BP, Cusack BJ, Knighton RA, Olson SJ, Mushlin PS, Olson RD. Daunorubicin cardiotoxicity: evidence for the importance of the quinone moiety in a free-radical-independent mechanism. Biochem Pharmacol 2000;60(10):1435-44.
- Shi H, Hudson LG, Liu KJ. Oxidative stress and apoptosis in metal ion-induced carcinogenesis. Free Radic Biol Med 2004;37(5):582-93.
- Shuai X, Ai H, Nasongkla N, Kim S, Gao J. Micellar carriers based on block copolymers of poly(epsilon-caprolactone) and poly(ethylene glycol) for doxorubicin delivery. J Control Release 2004;98(3):415-26.
- Sommer K, Kaiser S, Krylova OO, Kressler J, Pohl P, Busse K. Influence of amphiphilic block copolymer induced changes in membrane ion conductance on the reversal of multidrug resistance. J Med Chem 2008;51(14):4253-9.
- Thannickal VJ, Fanburg BL. Reactive oxygen species in cell signaling. Am J Physiol Lung Cell Mol Physiol 2000;279(6):L1005-28.
- Upadhyay K, Agrawal H, Upadhyay C, Schatz C, Le Meins J, Misra A, Lecommandoux S. Role of block copolymer nanoconstructs in cancer therapy. Crit Rev Ther Drug Carrier Syst 2009a;26(2):157-205.
- Upadhyay KK, Meins JF, Misra A, Voisin P, Bouchaud V, Ibarboure E, Schatz C, Lecommandoux S. Biomimetic Doxorubicin Loaded Polymersomes from Hyaluronan-block-Poly(gamma-benzyl glutamate) Copolymers. Biomacromolecules 2009b; Aug 5 (on Web).
- Xiong XB, Mahmud A, Uludağ H, Lavasanifar A. Conjugation of arginine-glycine-aspartic acid peptides to poly(ethylene oxide)-b-poly(epsilon-caprolactone) micelles

for enhanced intracellular drug delivery to metastatic tumor cells. Biomacromolecules 2007;8(3):874-84.

- Xiong XB, Mahmud A, Uludağ H, Lavasanifar A. Multifunctional polymeric micelles for enhanced intracellular delivery of doxorubicin to metastatic cancer cells. Pharm Res 2008;25(11):2555-66.
- Zheng C, Qiu L, Yao X, Zhu K. Novel micelles from graft polyphosphazenes as potential anti-cancer drug delivery systems: drug encapsulation and in vitro evaluation. Int J Pharm 2009;373(1-2):133-40.